Journal of
Colloid Science and Biotechnology
Vol. 1, 33–41, 2012

RESEARCH ARTICLE

Interaction Between Polyethyleneimine and Zwitterionic Surfactant: Effect on Association Processes in Bulk and Deposition onto Solid Wafers

S. E. Heisig, M. D. Merchán, and M. M. Velázquez*

Departamento de Química Física, Facultad de Ciencias Químicas, Universidad de Salamanca, 37008, Salamanca, Spain

Fluorescence probing and ζ-potential measurements have been used to characterize the interactions in bulk between the zwitterionic surfactant 3-[(3-cholamidopropyl)-dimethyl-ammonium]-1-propanesulphonate, CHAPS and the polymer polyethylene imine, PEI. Results show that the strongest attractive interactions are produced between the surfactant and the neutral form of the polymer PEI. Because the zwitterionic surfactant CHAPS has been proposed as component of biosensors, we are interested to study the effect of the polymer on CHAPS films, therefore we transfer the surfactant and PEI/CHAPS mixtures from the solution onto mica by using the Langmuir-Schaefer and dipping methodologies. The morphology of films is analyzed by means of Atomic force microscopy, AFM, Optical microscopy and Micro-Raman spectroscopy. The hydrodynamic flow of water after its evaporation induces the formation of ring-based structures not available to fabricate devices. This process predominates when materials are transferred from the solution onto mica by dipping. In contrast, the Langmuir-Schaefer films consist of spherical aggregates and the densest and the most ordered films were obtained by transferring the PEI/CHAPS mixture of surfactant concentration above the CMC.

Keywords: CHAPS, Polyethylene Imine, Zeta Potential, Langmuir-Schaefer, Dipping Method, AFM, Micro-Raman Spectroscopy.

1. INTRODUCTION

The zwitterionic surfactant 3-[(3-cholamidopropyl)-dimethyl-ammonium]-1-propanesulphonate (CHAPS) combines the properties of sulfobetaine-type surfactants and bile salts anions and it is widely used in biochemical applications such as protein solubilization[1] or disaggregation,[2] and as eluting agent in separation processes to provide selectivity.[3,4] Despite the extensive research on micellization or adsorption of CHAPS found in the literature,[5–12] there is limited research pertaining to mixtures with other surfactants[11] or with polymers.[13] However, it is well established that the presence of polymers in surfactant solutions decreases the critical micellar concentration (CMC), increases the surfactant adsorption at the interfaces and increases the ability of micelles to solubilise organic materials.[14,15] The synergistic effect is always stronger in oppositely charged systems; therefore there is no dearth of articles in the literature that addresses the interaction between polyelectrolytes and oppositely charged surfactants.[14,15] In contrast, the interaction between zwitterionic surfactants and polymers has received far less attention[16,17] despite its lower toxicity to humans and the environment than ionic surfactants.[18] It is well known that zwitterionic surfactants interact preferably with negatively charged molecules.[16,17,19,20] However, in a previous work carried out by our group, we have demonstrated the existence of attractive interactions between the zwitterionic surfactant CHAPS and the polycation Poly (diallyl-dimethil-ammonium chloride), PDADMAC. The results did not allow establishing the origin of this interaction.[21] In this paper, we study the interaction between the surfactant CHAPS and the polymer polyethyleneimine (PEI), because this polymer contains amine groups, which can exist in its neutral or cationic forms.

Recently, the zwitterionic surfactant CHAPS has been proposed as component of biosensors.[22] One important characteristic of the biosensors is that the analyte molecules have to be immobilized onto solids to react with the sensing component; therefore thinner films with a well-defined structure and good quality must be obtained to

*Author to whom correspondence should be addressed.

host the analyte molecules. When biomolecules, i.e., proteins, whose biological activity depends on the molecular arrangements, are immobilized on films, the control on the structure and orientation of the surface and the properties of molecules adsorbed on the solid wafers become extremely important.[23] In the preparation of well-defined films containing proteins, it is necessary to consider that the proteins for immobilization are aggregated in the solution avoiding the accurate orientation of molecules. To disaggregate proteins, ionic surfactants are often added to solutions. However, the ionic surfactants can modify the protein structure and its binding capacity to the sensing component; therefore zwitterionic surfactants such as CHAPS were proposed to substitute the ionic surfactants because they are less denaturing and more efficient than the non ionic ones at overcoming protein-protein interactions.[22, 24, 25] Another aspect of significance to construct solid biosensors is the deposition methodology. Several techniques such as dipping, Langmuir-Blodgett (LB) or Langmuir-Schaeffer (LS) can be used for this purpose. LB offers the possibility of preparing reproducible and homogeneous films with a high control of the interparticle distance.[26] However, in the case of rigid Langmuir monolayers such as proteins, the LB technique does not achieve good transference ratios due to the poor molecular reorganization of molecules on the subphase surface. The Langmuir-Schaeffer methodology has been proposed to solve this problem. In the LS technique, the position of the solid substrate is parallel to the interface and there is no requirement of reorientation. Using the LS methodology a great number of proteins and other rigid layers have been successfully deposited.[27]

One inexpensive methodology of deposition on solids is the dipping method. In this method, the solid substrate is dipped vertically into the suspension containing proteins and held for a given time to eliminate the interface fluctuations. Finally, the dipped solid substrate is subsequently extracted vertically from the suspension.[28] It is interesting to note that the drying of a liquid with suspended material on a solid surface leaves different structures.[29–31] Several researchers have utilized this process for self-assembly of materials such as single-walled nanotubes (SWNT)[32, 33] or graphene flakes.[34] The results obtained showed that the structure of the nanomaterials after liquid evaporation depends on the nature of the contact lines during the evaporation, which is a function of the properties of nanoparticles (size and concentration) and of the evaporation environment (relative humidity and rheological properties of the evaporating liquid). Accordingly, we study the effect of two different deposition methodologies on the morphology of films prepared with the zwitterionic surfactant CHAPS. Langmuir-Schaefer and dipping methodologies were chosen. The first one was chosen because, to the best of our knowledge, it has not been proposed to construct high-quality films of CHAPS and the second one was used for comparative purposes because it has been employed for the fabrication of sensors containing the surfactant CHAPS.[22, 24, 25] Finally, we study the effect of the polymer PEI on the morphology of films with CHAPS by transferring mixtures of PEI/CHAPS from the aqueous solutions onto mica.

The remaining sections of this paper are organized as follows: the next section contains experimental details and description of methodologies and techniques. In the results and discussion section we study the interactions of CHAPS and PEI by determining the Critical Aggregation Concentration (CAC) of surfactant-polymer micelles at different pH. The ζ-potential for aggregates with different polymer compositions at CAC concentrations of surfactant are also presented in this section. In the second part of this section, the morphology of films of CHAPS and CHAPS/PEI mixtures deposited on mica by Langmuir-Schaefer and dipping methodologies are analyzed by using AFM, optical microscopy (OM) and Micro-Raman spectroscopy. Finally, the main conclusions are presented.

2. MATERIALS AND METHODS

2.1. Materials

The surfactant CHAPS (SigmaUltra TLC), the polyelectrolyte branched polyethyleneimine, PEI ($M_r = 2$ kDa), and the fluorescent probe, pyrene were obtained from Sigma-Aldrich, used as received and stored under vacuum. The polymer molecular weight was provided by the manufacturer. 1 M HCl was added to the polymer solutions to obtain pH values of 3 and 7 from a pH value of 10 of PEI in water. The substrate muscovite (mica) quality V-1 was supplied by EMS (USA). The mica surface was freshly cleaved before use.

The solutions were prepared with water purified with RiOs and Milli-Q systems from Millipore having a conductivity of 0.2 μS/cm. The polymer solutions were prepared using a gravimetric technique. The surfactant was then dissolved in a known polymer concentration.

Incorporation of pyrene into micelles was performed as follows: an appropriate volume of pyrene dissolved in methanol was poured into a volumetric flask and the solvent was evaporated. The solutions of surfactant or polymer-surfactant mixtures were added to the evaporated residue, and the solution was stirred until the fluorescence probe was dissolved. The pyrene concentration was kept constant at 2.0 μM.

2.2. Methods

2.2.1. Steady State Fluorescence Measurements

The emission spectra of pyrene incorporated on surfactant or polymer-surfactant mixtures were recorded with an LS-50B spectrofluorometer from Perkin-Elmer. The

excitation wavelength was 319 nm and the excitation and emission slits were kept constant at values of 5/5 nm or 7/7 nm as a function of the fluorescence intensity. All spectra were recorded at 25 °C.

2.2.2. Zeta-Potential Analyzer

The electrophoretic mobility measurements were carried out by means of the laser Doppler electrophoresis technique using the Zetasizer Nano ZS device (Malvern, UK). The equipment uses a He-Ne-laser at 5 mW and 633 nm. All experiments were performed in a DTS 1060C clear disposable zeta cell. The electrophoretic mobility, μ_e, was measured at 25.0 °C and converted into zeta-potential, ζ, using the Smoluchowski's relation, $\zeta = (\mu_e \eta)/\varepsilon$ where η and ε are the viscosity and the permittivity of the solvent, respectively. Each reported value is an average over thirty measurements and the standard deviation of these measurements was determined to ascertain the extent of the experimental error.

2.2.3. Surface Tension Measurements

A drop tensiometer model TVT-2 from Lauda[35] employing the dynamic method was used to measure the dynamic surface tension above 10 s. The inner radius of the steel capillary was 1.345 mm and the employed syringe was 5 ml. The best conditions to ensure the correct determination of the equilibrium surface tension values have been chosen using criteria published elsewhere.[19, 36]

All measurements were performed at 25.0 °C. Temperature in the tensiometer was controlled by means of thermostat/cryostat RM 6.

2.2.4. Film Deposition

Surfactant-polymer mixtures were deposited onto mica by using the Langmuir Schaefer method with a KSV2000 System 2 and the Langmuir Schaefer holder KN 0006 from KSV (KSV, Finland). Since measurements were carried out in soluble monolayers, the equilibrium surface tension values were simultaneously measured until they reached the equilibrium value. Then the deposition was started. Surface tension measurements showed that the surface tension was reduced after the addition of 1% PEI from 50.5 mN/m to 48 mN/m for 2 mM CHAPS solutions and from 46 to 44 mN/m for CHAPS solutions with surfactant concentration of 10 mM. The temperature was maintained at (25.0 ± 0.1) °C by flowing thermostated water through a jacket at the bottom of the trough. The temperature near the surface was measured with a calibrated sensor from KSV. The water temperature was controlled by means of thermostat/cryostat Lauda Ecoline RE-106.

The dipping method consists of dipping vertically a clean mica substrate into the surfactant or surfactant-polymer solutions at 25 °C at a rate of 11 mm/min to a depth of 15 mm and then holding for 10 min to eliminate interface fluctuations. The dipped substrate was subsequently extracted at a rate of 11 mm/min.

2.2.5. Atomic Force Microscopy (AFM)

AFM images from films transferred on mica substrates were obtained in constant repulsive force mode using an AFM (Nanotec Dulcinea, Spain) with a rectangular microfabricated silicon nitride cantilever (Olympus OMCL-RC800PSA) having a height of 100 μm, a Si pyramidal tip and a spring constant of 0.73 N/m. The scanning frequencies were usually in the range between 0.5 and 2.0 Hz per line. The measurements were carried out under ambient laboratory conditions.

2.2.6. Optical Microscopy

Optical microscopy images were obtained in a ZEISS Axio Imager Mim provided with six objectives connected to a digital camera.

2.2.7. Raman Spectroscopy

Raman spectra were acquired with a dispersive Jobin-Yvon LabRam HR 800 spectrometer coupled with an optical microscope Olympus BXFM. CCD was used as detector and cooled at −70 °C. Laser used was 532 nm with 3 mW of power on samples. Microscope objective was 100×.

3. RESULTS AND DISCUSSION

3.1. Interactions Between CHAPS and PEI in Solution

The study of surfactant-polymer interactions is usually carried out by determining the CMC of micelles in the absence and presence of polymer PEI. The CMC of a surfactant can be determined by the appearance of a discontinuity in the variation of some properties in solution as a function of surfactant concentration. In this work, we use the change in the fluorescence emission spectrum of pyrene. This method is based on the variation of the intensity of the vibrational bands of pyrene emission corresponding to wavelengths of 372 and 382 nm, expressed as the I_1/I_3 ratio. The I_1/I_3 ratio decreases when the polarity in the environment of the probe decreases.[37, 38]

The ratio of I_1/I_3 as a function of the surfactant concentration is shown in Figure 1. Each curve corresponds to mixtures with the polymer concentration kept constant. The range of polymer concentrations analyzed was 0.1 to 1 wt%. The value represented at the surfactant concentration of 1×10^{-4} M, corresponds to the I_1/I_3 ratio of the probe in each medium. Curves in Figure 1 show two break points, the first one is at surfactant concentration corresponding to CAC, and the second one to CMC, respectively. It is well established that the CAC is the surfactant

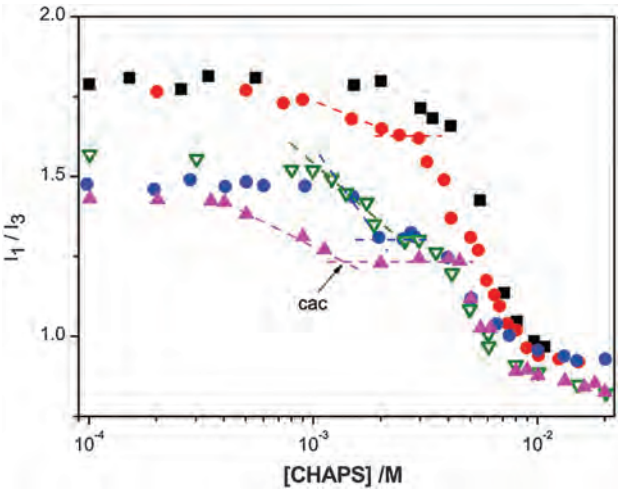

Fig. 1. Effect of PEI concentration on the Plot of the I_1/I_3 ratio of the pyrene fluorescence spectrum against the CHAPS concentration for (solid black squares) aqueous solutions; (red circles) 0.1% wt PEI; (green triangles) 0.5% wt PEI; (blue circles) 0.7% PEI and (magenta triangles) 1% wt PEI. All measurements were performed at 25 °C.

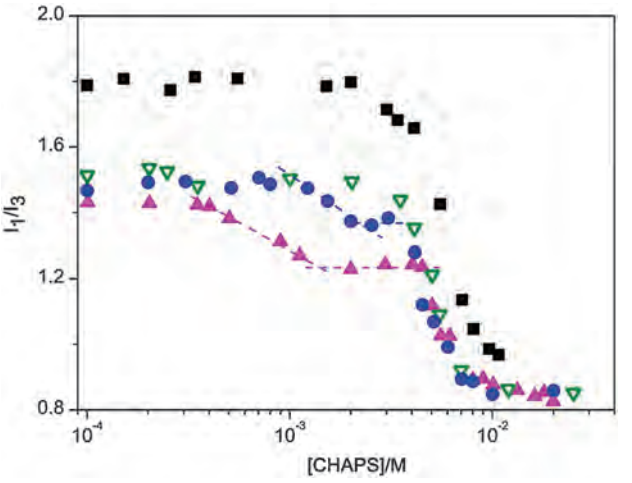

Fig. 2. Effect of pH on the plot of the I_1/I_3 of the pyrene fluorescence spectrum against the CHAPS concentration at 1% wt PEI for (magenta triangles) aqueous solution, pH = 10; (blue circles) pH = 7; (open green triangles) pH = 3 and (solids black square) CHAPS without polymer. All measurements were performed at 25 °C.

concentration above which hydrophobic domains of surfactant and polymer are formed, while the CMC corresponds to a surfactant concentration at which micelles of surfactant in water are formed after the saturation of polymer by the surfactant molecules. The CAC was determined from the curves as the concentration at which I_1/I_3 becomes constant following a sharp decrease. Results are shown in Table I. It is evident from the table that the CAC values are lower than the CMC of the surfactant in water and decreases as the polymer concentration increases. This expected result means that the surfactant molecules prefer to micellize with polymer molecules than with themselves.

To establish the origin of the interactions between the surfactant and polycation molecules, we determined the CAC of mixtures at different pH. We studied the behavior of CHAPS in 1 wt% PEI because it is the concentration at which the system presents a stronger interaction. According to the pK_a values of PEI[39] in aqueous solutions, at pH 7 all the primary and secondary amines are in their protonated form and at pH 3, the tertiary ones are protonated too. Figure 2 shows the plot of I_1/I_3 against the surfactant concentration for the mixtures at pH 3, 7 and 10. Also CHAPS in water curve is included in Figure 2 for better comparison. As in Figure 1, the values of I_1/I_3 represented at 1×10^{-4} M are the values of the probe at 1 wt% PEI and the selected pH.

In Figure 2, we can observe that the curves corresponding to mixtures at pH 3 and CHAPS in water are quite similar and present only a break point at the CMC of the surfactant CHAPS. However, the curve for mixtures prepared at pH 7, shows a plateau at 2.2 mM, shorter than the plateau observed in the pH 10 curve at 1.4 mM. From Figure 2, it is possible to conclude that the interaction becomes weaker when the polymer is more charged. This is consistent with the weaker interaction observed between zwitterionic surfactants and cationic molecules.[21,40] Thus, when the pH decreases to a value of 3 and the amines of polymer are completely protonated, no interactions are detected. It is necessary to note that in mixtures between CHAPS and the polycation PDADMAC attractive interactions were observed;[21] the opposite behavior observed in the present work can be interpreted as the differences in spatial conformation when the molecule is protonated. Those changes have been observed in PEI molecule when the pH changes from 3 to 7.[41] Thus, from our results it is possible to conclude that the charged amine groups of PEI are not available to the negative part of the zwitterionic surfactant CHAPS. On the contrary, in aqueous solutions, interactions between the surfactant and the neutral form of the polymer become significant, decreasing the CAC from 6.8 mM (CHAPS in water) to 1.4 mM. We can conclude that while PEI is in its neutral form, van der Waals interactions becomes more important than the electrostatic ones and a significant interaction between CHAPS and PEI is observed, and while the PEI is getting more charged the interactions become weaker.

Table I. CAC values of CHAPS-PEI mixtures at different PEI concentrations determined by steady state fluorescence of pyrene, and CMC value of CHAPS in aqueous solution. ζ-potential of CHAPS-PEI aqueous mixtures, [CHAPS] = 2.0 mM at different PEI concentrations, and PEI 1% wt at pH = 7.

PEI (%wt)	CAC/mM	ζ-potential/mV
0	6.8 (CMC)	-5.0 ± 0.4
0.1	2.4	-5.4 ± 0.3
0.5	2.4	-4.3 ± 0.2
0.7	2.2	-3.4 ± 0.2
1	1.4	-6.6 ± 0.4
1 (pH = 7)	2.2	—

3.2. Electrophoretic Mobility Results

To study the effect of the polymer on the electric properties of micelles composed by PEI and CHAPS, we determined the electrophoretic mobility of CHAPS-PEI mixtures in aqueous solution. We select this system because it presents the strongest interaction between the polymer and surfactant molecules. We did not obtain the electrophoretic mobility of solutions with pH 3 and 7 because we obtained the acid pH by adding HCl. This fact modifies the electric potential of the polymer molecules and the main differences observed after the formation of mixed micelles are smaller enough to obtain conclusive results.

We carried out the electrophoretic mobility measurements at a surfactant concentration of 2 mM in which the mixed micelles predominate. The values are shown at Table I. The ζ-potential average value obtained for 2.0 mM of CHAPS is in agreement with the value obtained in a previous work. In that work, the values obtained with different surfactant concentrations were independent of the surfactant concentration and the average value found was -5 mV.[21] ζ-potential average values of mixed micelles of PEI and CHAPS shown in Table I do not depend on the PEI concentration and are quite similar to the values of CHAPS in water, as expected because PEI is in its neutral form.

In order to obtain information of the effect of polymer addition on aggregates size, dynamic light-scattering experiments have been performed.[42] However, it was no possible to obtain information from these measurements because the relaxation time of the fastest process for polymer solutions is close to the value corresponding to CHAPS micelles. Accordingly, it cannot separate the different components of the multimodal autocorrelation functions found for solutions with polymer and surfactant molecules mixtures because the time relaxations corresponding to the polymer and micelles are close enough.

3.3. CHAPS Films Obtained by Dipping and Langmuir-Schaefer Methods

We transferred the surfactant CHAPS from solutions with surfactant concentrations below and above the CMC onto mica by using two techniques, dipping and Langmuir-Schaefer. After deposition, the films were dried at room temperature and the morphology of the surfactant films was analyzed by AFM and OM. Figure 3(a) presents a representative AFM image of CHAPS deposited on mica by dipping in aqueous solution. The surfactant concentration was 10 mM; this value is above the CMC. Figures 3(b) and (c) show higher magnification AFM images and the roughness of the film, respectively. As can be seen in figures 3a and 3b, surfactant molecules form ring-shaped patterns. This phenomenon is observed everyday when liquids drops with solutes evaporate, and is commonly known

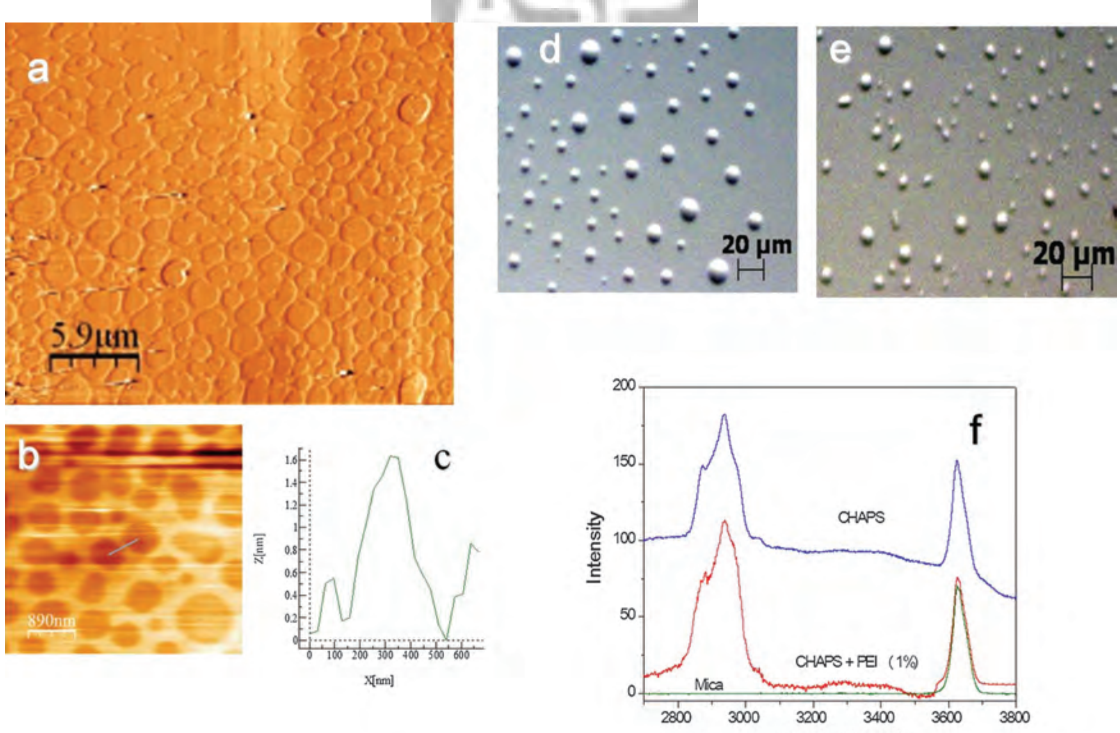

Fig. 3. (a) and (b) AFM images of CHAPS films constructed by dipping. (c) Roughness of the film showed in (b). The surfactant concentration was 10 mM. (d) and (e) OM images of CHAPS films constructed by the LS methodology; CHAPS concentration was 2 mM and 10 mM respectively. (f) Micro-Raman spectra of mica and LS films of CHAPS (2 mM) and mixtures of CHAPS (2 mM) with PEI 1% wt.

as coffee ring phenomenon, and is due to induced capillary flow.[29–31] We analyze the chemical composition of the different regions by obtaining the micro-Raman spectrum from 2400 to 3800 cm^{-1}. The Raman spectrum of the ring patterns contains bands centered between 2850–2950 cm^{-1}, characteristic of symmetric and antisymmetric stretching of CH groups of the surfactant and three bands centered at 3030, 3280 and 3400 cm^{-1} ascribed to the sulphonate, and the stretching bands of the hydroxyl groups of CHAPS.[43] The Micro-Raman spectrum recorded on the ring hole presents a band centered at 3620 cm^{-1}, corresponding to the hydroxyl groups of the mica (see Fig. 3(f)). This indicates that no material is deposited in this region. Similar behaviour is observed for solutions with surfactant concentration below the CMC. The roughness obtained from AFM of the ring patterns is independent of the surfactant concentration and the average value found is 1.5 nm.

Figures 3(d) and (e) show the OM images of the CHAPS films constructed by the LS methodology. The films were transferred from the interface of solutions with surfactant concentrations below and above the CMC (2 mM and 10 mM), respectively. By analyzing the AFM and OM images it is possible to conclude that the morphology of domains is independent on the surfactant concentration. To gain insights into the chemical composition of the spherical aggregates, we recorded the micro-Raman spectrum inside them. A representative spectrum is presented in Figure 3(f). The Raman spectrum inside the aggregates contains bands characteristic of the surfactant CHAPS, while outside the aggregates, the Raman spectrum corresponds to the solid wafer, mica. We also determine the roughness by AFM and the value found, 1.9 nm, is very close to the roughness of the CHAPS film deposited by dipping.

Comparison between the morphology of films prepared by dipping and LS allow us to conclude that deposition by LS method gives spherical aggregates homogeneously distributed on the solid, while with the dipping procedure, the ring structures predominate on the solid. The differences can be explained considering that the ring structures are induced by the water evaporation, dewetting process.[29–31] This is a very important process when the solid is dipped into the surfactant solutions, because a layer containing water is deposited on the solid among the particles dissolved in the solutions. However, different situation occurs when films are directly transferred from the interface onto the solid using the LS methodology. In this case, only a small amount of water is transferred on the solid, demonstrating that this small water concentration cannot induce significant dewetting processes.

To study the effect of the polymer PEI on the morphology of CHAPS films, we selected the surfactant-polymer mixtures with the strongest attractive interactions. Therefore, we transferred two different mixtures with surfactant concentrations at the CAC and above the CMC dissolved in aqueous solution of 1 wt% PEI.

Figure 4(a) shows the OM image of a PEI/CHAPS film prepared by the LS method at the CAC. If one compares the morphology of aggregates in this film with the morphology of aggregates obtained by LS for CHAPS without polymer, Figure 3(d), it can be seen that the structures

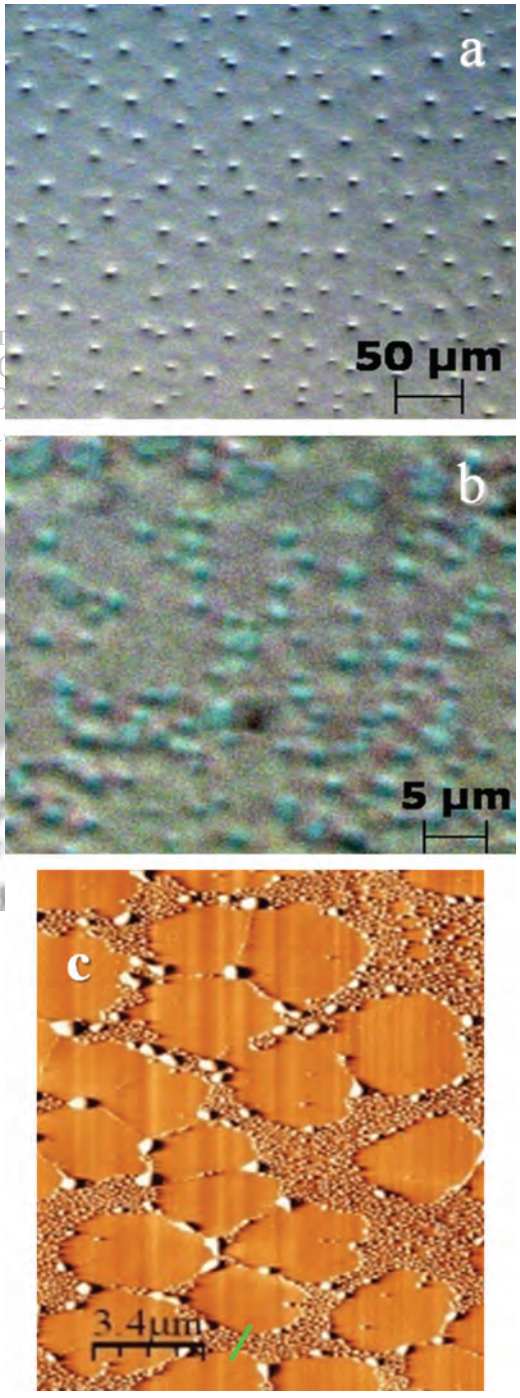

Fig. 4. Mixtures of CHAPS 2 mM with 1% wt. PEI. OM Images of films constructed by: (a) LS and (b) dipping. (c) AFM image of the film presented in (b).

are quite similar. We also compared the Raman spectra recorded for samples of CHAPS with and without PEI, in Figure 3(f). For the sake of clarity the spectrum of CHAPS was shifted in the intensity scale. As can be seen, the characteristic bands of the surfactant are observed in both, and no new bands appear in these spectra. This fact seems to indicate that the surfactant molecules predominate in the film obtained from solutions of PEI and CHAPS at the CAC. Taking into account that in the LS method, the molecules are transferred from the air-water interface onto the solid, the results are consistent with the idea that the surfactant molecules are the main component of the interfaces at the CAC.[44]

The AFM and OM images of films obtained by dipping mica in the polymer-surfactant solutions at the CAC are presented in Figures 4(b) and (c) respectively. The images show the formation of ring patterns. However, the morphology of the rings is different to that for CHAPS films. Thus, if we compare the images of the two films (see Figs. 3(a) and 4(b and c)), it is possible to see that deposition of polymer-surfactant mixtures gives spherical aggregates at the edge of a flat domain, while the films constructed with CHAPS in water do not present these aggregates. The roughness of the flat domain is around 35 nm and increases until 60 nm for the spherical aggregates. The high roughness values of films with polymer contrast with the roughness of CHAPS films (1.9 nm). To interpret these differences, it is necessary to consider that at the CAC, hydrophobic domains of surfactant and polymer molecules in bulk are formed[44–47] and consequently, can be transferred onto a solid by using the dipping methodology. When the surfactant concentration is increased above the CMC, the images show well-ordered spherical aggregates (see Figs. 5(a and b)). We also presents as inset in Figure 5(c), a representative image of these films obtained by Micro-Raman spectroscopy. The roughness of aggregates was 125 nm; this value is higher than the one calculated for PEI/CHAPS mixtures with surfactant concentration at the CAC. The Micro-Raman spectra were recorded inside and outside the aggregates. Two representative spectra are collected in Figure 5(c). For comparative purposes, in Figure 5(c) is also represented the Raman spectrum of PEI (1%) deposited by dipping. The Raman spectrum inside the aggregates is similar to the one recorded for CHAPS (Fig. 3(f)), while the spectrum outside the aggregates shows similarity with that of PEI. Thus, our results seem to indicate that the aggregates are mainly constituted by CHAPS, and the PEI molecules

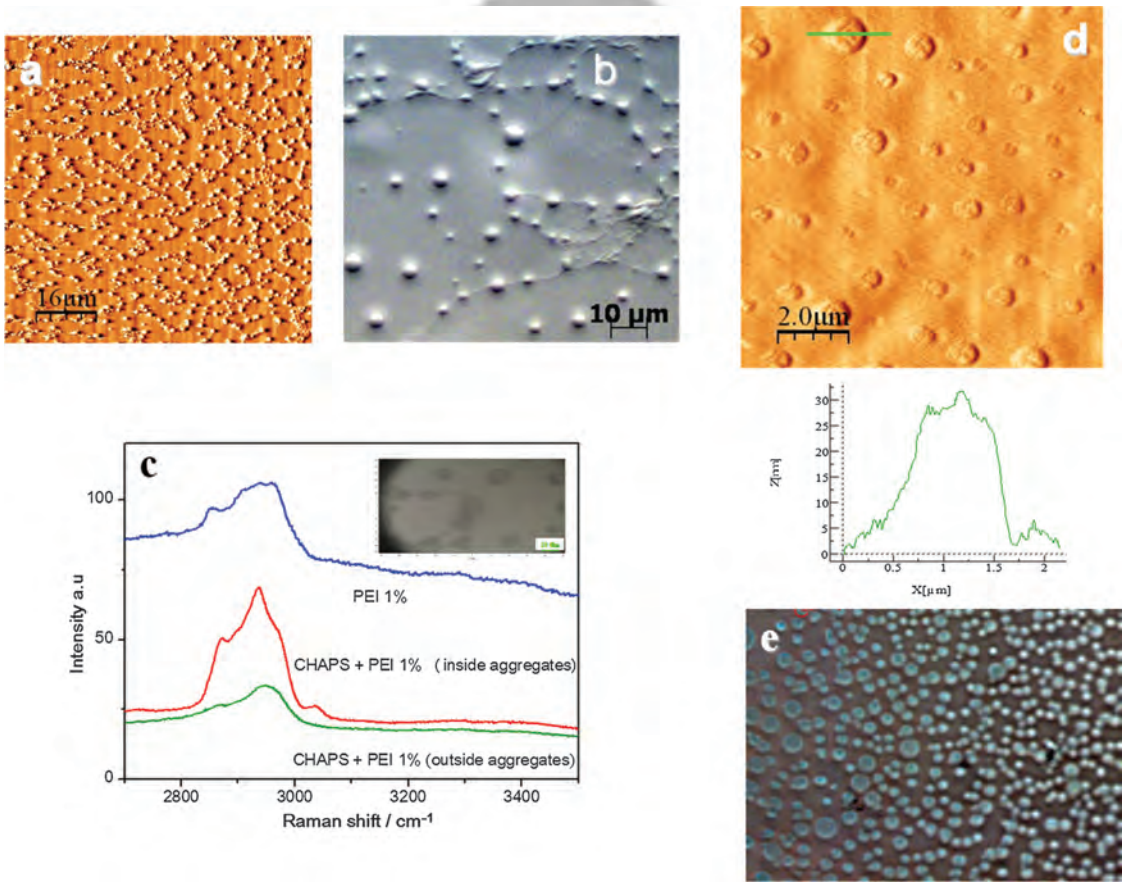

Fig. 5. Mixtures of CHAPS 10 mM with 1% wt. PEI. AFM (a) and OM (b) images of films constructed by dipping. (c) Micro-Raman spectra of different films prepared by dipping. AFM (d) and OM (e) images of films transferred by LS methodology.

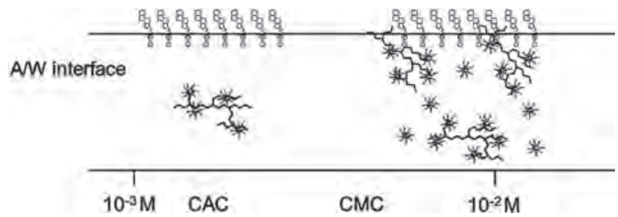

Fig. 6. Possible structures of PEI/CHAPS aggregates with increasing CHAPS concentration. The multilayered structure at high concentration has been previously proposed.[44, 45]

outside them could induce orientation of the aggregates on the film.

Finally, the AFM and OM images of LS films obtained by transferring the monolayer adsorbed at the interface of the PEI/CHAPS solutions at the CMC are shown in Figures 5(d) and (e). The images show big aggregates of roughness around 30 nm. The presence of big aggregates of polymer surfactant complexes at the interface has been proposed by other authors.[44–47] In our system, we have demonstrated that PEI/CHAPS complexes do not bear electric charge and consequently, present high surface activity. This behavior promotes its presence at the air-water interface and the subsequent transference onto mica. To illustrate our results a scheme of the possible structures of PEI/CHAPS aggregates are shown in Figure 6. The Raman spectra recorded on different regions allows us to detect well-defined domains of PEI and CHAPS molecules. Thus, the region between the aggregates mainly contains PEI molecules while CHAPS molecules predominate in the aggregates. This behavior is quite similar to that observed for films prepared with this solution by dipping.

4. CONCLUSIONS

The results found in this work demonstrate that the attractive interaction between the polymer PEI and the surfactant CHAPS in bulk strongly depend on the polyelectrolyte charge. Thus, the strongest interaction was observed between neutral polymer molecules and the surfactant. This fact seems to indicate that the interaction is of van der Waals origin. In order to use the surfactant CHAPS supported on mica as pattern for biosensors, we transferred the surfactant onto mica by using two different methodologies, dipping and Langmuir-Schaefer. Results demonstrate that by using the dipping method, ring-based structures are formed on the solid. These structures are due to the hydrodynamic flow of water after its evaporation. Since ring-shaped patterns are not easily incorporated into complex electrical devices,[30] this methodology cannot be used to construct these devices. The addition of PEI modifies the ring structure and the most important changes are observed when the mixtures contain the surfactant concentration above the CMC and PEI concentration of 1% wt. The Langmuir-Schaefer method avoids the formation of ring-shaped structures and allows transferring spherical aggregates from the air-water interface onto mica. The densest and most ordered film is obtained by transferring the mixture of CHAPS and PEI (1%) with surfactant concentration above the CMC.

Acknowledgments: The authors thank financial support from ERDF and MEC (MAT 2010-19727). We thank to Drs Cirera and Claramunt (University of Barcelona) for the Micro-Raman facility.

References and Notes

1. A. Chattopadhyay and K. G. Harikumar, *FEBS Lett.* 391, 199 (**1996**).
2. A. J. Dingley, J. P. Mackay, B. E. Chapman, M. B. Morris, P. W. Kuchel, B. D. Hambly, and G. F. King, *J. Biomol. NMR* 6, 321 (**1995**).
3. (A) J. J. Buckley and D. B. Wetlaufer, *J. Chromatogr.* 464, 61 (**1989**); (B) *J. Chromatogr.* 518, 111 (**1990**).
4. L. J. J. Hronowski and T. P. Anastassiades, *Anal. Biochem.* 191, 50 (**1990**).
5. R. E. Stark, P. D. Leff, S. G. Milheim, and A. Kropf, *J. Phys. Chem.* 88, 6063 (**1984**).
6. T. Schürholz, J. Kehne, A. Geiselmann, and E. Newmann, *Biochemistry* 31, 5067 (**1992**).
7. T. Shürholz, *Biophys. Chem.* 58, 87 (**1996**).
8. C. E. Giacomelli, A. W. P. Vermeer, and W. Norde, *Langmuir* 16, 4853 (**2000**).
9. K. Lunkenheimer, G. Sugihara, and M. Pietras, *Langmuir* 23, 6638 (**2007**).
10. H. Razafindralambo, C. Blecker, S. Delhaye, and M. Paquot, *J. Colloid. Int. Sci.* 174, 373 (**1995**).
11. (A) J. S. Ko, S. W. Oh, K. W. Kim, N. Nakashima, S. Nagadome, and G. Sugihara, *Colloids and Surf. B* 45, 90 (**2005**); (B) S. W. Oh, J. S. Na, J. S. Ko, S. Nagadome, and G. Sugihara, *Colloids and Surf. B* 62, 112 (**2008**).
12. M. A. Partearroyo, F. M. Goñi, I. A. Katime, and A. Alonso, *Biochem Int.* 16, 259 (**1988**).
13. D. Lasic, F. J. Martin, J. M. Neugebauer, and J. P. Kratohvil, *J. Colloid Interface Sci.* 133, 539 (**1989**).
14. E. D. Goddard and K. P. Ananthapadmanaban (eds.), Interactions of Surfactants with Polymers and Proteins, CRC Press, Boca Raton, FL (**1993**).
15. K. Holberg, B. Jönsson, B. Kronberg, and B. Lindman, Surfactant and Polymers in Aqueous Solutions 2nd edn., J. Wiley and Sons Chichester, West Sussex PO19 8SQ, England (**2003**).
16. R. Ribera and M. M. Velázquez, *Langmuir* 15, 6686 (**1999**).
17. C. Delgado, M. D. Merchán, and M. M. Velázquez, *J. Phys. Chem. B* 112, 687 (**2008**).
18. E. S. Basheva, D. Ganchev, N. D. Denkov, K. Kasuga, N. Satoh, and K. Tsujii, *Langmuir* 16, 1000 (**2000**).
19. D. López-Díaz, I. García-Mateos, and M. M. Velázquez, *Colloid. Surf. A* 270, 153 (**2005**).
20. D. López-Díaz, I. García-Mateos, and M. M. Velázquez, *J. Colloid. Int. Sci.* 299, 858 (**2006**).
21. M. D. Merchán and M. M. Velázquez, *Colloids Surf. A* 366, 12 (**2010**).
22. T. Lee, W. A. El-Said, J. Min, B. K. Oh, and J. W. Choi, *Ultramicroscopy* 110, 712 (**2010**).
23. A. P. Girart, S. Godoy, and L. J. Blum, *Adv. Colloid Interf. Sci.* 116, 205 (**2005**).

24. J. B. Lee, D. J. Kim, J. W. Choi, and K. K. Koo, *Mat. Sci. Eng. C* 24, 79 **(2004)**.
25. J. W. Choi, K. S. Park, W. Lee, B. K. Oh, B. S. Chun, and S. H. Paek, *Mat. Sci. Eng. C* 24, 79 **(2004)**.
26. M. C. Petty, Langmuir-Blodgett Films: An Introduction, Cambridge University Press: Cambridge **(1996)**.
27. C. Nicollini, Molecular Bioelectronics, World Scientific Pub. Co. Singapore **(1996)**.
28. S. H. Im, O. O. Park, and M. H. Kwon, *Macromolecular Research* 11, 110 **(2003)**.
29. R. D. Deegan, O. Bakajin, T. F. Dupont, G. Huber, S. R. Nagel, and T. A. Witten, *Nature* 389, 827 **(1997)**.
30. R. Sharma, C. Y. Lee, J. H. Choi, K. Chen, and M. S. Strano, *Nanolett.* 7, 2693 **(2007)**.
31. X. Shen, C. M. Ho, and T. S. Wong, *J. Phys. Chem. B* 114, 5269 **(2010)**.
32. R. Sharma and M. S. Strano, *Adv. Mater.* 21, 60 **(2009)**.
33. R. Duggal, F. Hussain, and M. Pasquali, *Adv. Mater.* 18, 29 **(2006)**.
34. C. J. Shih, A. Vijayaraghavan, R. Krshnan, R. Sharma, J. H. Han, M. H. Ham, Z. Jin, S. Lin, L. C. Paulus, N. F. Reuel, Q. H. Wang, D. Blanschtein, M. S. Strano, *Nature Nano* 6, 439 **(2011)**.
35. R. Miller, A. Hoffman, R. Hartman, K. H. Schano, and A. Halbig, *Adv. Mater.* 4, 370 **(1992)**.
36. C. Delgado, M. D. Merchán, M. M. Velázquez, and J. Anaya, *Colloid Surf. A* 280, 17 **(2006)**.
37. K. Kalyanasundaram, Photochemistry in Microheterogeneous Systems, Academic Press, Orlando **(1987)**.
38. K. Kalyanasundaram and J. K. Thomas, *J. Am. Chem. Soc.* 99, 2039 **(1977)**.
39. Y. Wang, P. Chen, and J. Shen, *Biomaterials* 27, 5292 **(2006)**.
40. X. L. Zhang, D. J. F. Taylor, R. K. Thomas, and J. Penfold, *J. Coll. Int. Sci.* 356, 647 **(2011)**.
41. G. M. Lindquist and R. A. Stratton, *J. Coll. and Int. Sci* 55, 45 **(1976)**.
42. M. M. Velázquez, M. Valero, F. Ortega, and J. B. Rodríguez González, *J. Colloid Interf. Sci.* 316, 762 **(2007)**.
43. N. B. Colthup, L. H. Daly, and S. E. Wiberley, Introduction to IR and Raman spectroscopy, 2nd edn., Academic Press, New York **(1975)**.
44. D. J. F. Taylor, R. K. Thomas, and J. Penfold, *Langmuir* 18, 4748 **(2002)**.
45. C. Monteux, C. E. Williams, J. Meunier, O. Anthony, and V. Bergeron, *Langmuir* 20, 57 **(2004).**
46. C. Monteux, C. E. Williams, J. Meunier, O. Anthony, and V. Bergeron, *Langmuir* 20, 5358 **(2004)**.
47. C. Monteux, C. E. Williams, J. Meunier, O. Anthony, and V. Bergeron, *Langmuir* 20, 5367 **(2004)**.

Received: 29 February 2012. Accepted: 15 March 2012.